

# THE EFFECT OF SHEARED TOROIDAL FLOW ON AN FRC'S $n=2$ ROTATIONAL INSTABILITY

Edward L. Ruden

Air Force Research Laboratory, Directed Energy Directorate

A Field Reversed Configuration (FRC) is observed to gain angular momentum until  $\alpha = \Omega_R/\Omega_{Di}$  (rotational frequency over ion diamagnetic drift frequency) reaches a critical value, at which point an instability with azimuthal mode number  $n = 2$  develops. Questions remain as to whether the observed threshold is explained by published calculations, which assume a rigid rotor profile. Questions also remain as to the cause of the spin-up, but it necessarily involves angular momentum transport to the FRC through the outer surface. Rotation of the bulk, then, via kinematic viscosity and/or convection can entail significant velocity shear. Rotation results in plasma (centripetal) acceleration supported by an external magnetic field, so the instability may be interpreted as a Rayleigh-Taylor (R-T) mode. Both sheared flow and Finite Larmor Radius (FLR) effects are recognized as mitigating factors for the R-T instability, and the two effects are synergistic.

The rotational instability is investigated here using an analytic planar R-T model of an FLR plasma with a magnetically transverse sheared flow layer accelerated by the magnetic field. One result is that if the sheared layer is too thin to reach the magnetic (reversal) axis, it is unstable. The coupling between gyroviscosity and flow shear in this case negates the stabilizing effect of both within a range of modes, and convection of the sheared layer to the magnetic axis can be expected to occur quickly. Once this happens, though, the FRC is stable until the shear factor reaches a high value, at which time the  $n = 2$  mode goes unstable. Technically,  $n = 1$  goes unstable first, but the (planar) model applied to cylindrical geometry does not conserve lateral linear momentum for this mode, so is inapplicable.

This model provides insight into what may be an important feature of FRC stability, although less simplified calculations are needed. Nonetheless, it can be used tentatively to predict stability characteristics of an FRC during compression by an electromagnetically imploded metal cylinder (for Magnetized Target Fusion adiabatic compression). This is of concern since acceleration from such an implosion supplements centripetal acceleration, and  $\alpha$  increases by a factor of 2.4, assuming angular momentum conservation, adiabatic compression, and the theoretical volume vs. radius scaling.

## Introduction

Simulations to date of the  $n = 2$  rotational instability in  $\theta$  pinches using FLR MHD[1] and Vlasov[2] models, and in elongated FRC's using a hybrid model[3] generally assume the plasma rotates with a rigid rotor profile. The former two imply stability for  $\alpha \lesssim 1.2$ – $1.5$  for  $\theta$  pinches. The hybrid FRC simulations, though, imply  $n = 2$  requires  $\alpha \lesssim 0.4$  for stability. Harned suggests that the FRC's lower critical  $\alpha$  may be attributable to resonant ions near the magnetic axis due to the magnetic field vanishing there (an effect not present in a  $\theta$  pinch nor representable by the FLR stress tensor). It is argued here, though, that the FRC's different density profile may play at least as great a role. Regardless, the discrepancy with the experimental stability criterion[4] of  $\alpha \lesssim 1.0$ – $1.2$ , is not well explained. The purpose of this paper is to pose a hypothesis for this discrepancy supported by a simple analytic model and heuristic considerations, pending more detailed analysis.

Little consideration is given in the aforementioned studies as to how a rigid rotor profile develops. The equilibration time scale for attaining rigid rotor status by viscous drag is

$$\tau_{\Omega} = \frac{(r_s - r_0)^2}{\nu_k} \quad \nu_k \left( \frac{\text{m}^2}{\text{sec}} \right) = \frac{3.4 \times 10^2 A_i Z^2 \ln \Lambda}{(ZT_e + T_i)\sqrt{T_i}} \quad (1)$$

where  $r_s$  and  $r_0$  are the separatrix and magnetic axis radii, respectively,  $\nu_k$  is kinematic viscosity[5],  $Z$  is mean ionization level,  $T_i$  and  $T_e$  are ion and electron temperatures in eV, respectively,  $\ln \Lambda$  is the Coulomb logarithm, and  $A_i$  is the ion atomic mass in amu. For a  $\text{D}_2$  plasma with  $r_s - r_0 = 1$  cm,  $T_i = T_e = 200$  eV, and  $\ln \Lambda \approx 15$ , typical of MTF FRC's[6],  $\tau_{\Omega} \approx 83 \mu\text{s}$ . An  $n = 2$  instability, though, is observed to develop within  $15 \mu\text{s}$  of formation. Faster angular momentum transport schemes have been proposed[7]. Indeed, in this paper a mechanism is proposed whereby a sheared flow layer establishes itself between  $r_s$  and  $r_0$  on an MHD time scale by convection resulting from the instability of any initially thin sheared layer. Once this happens, though, a stable shear flow pattern emerges until the characteristic angular velocity  $\Omega_R$  reaches a critical value. Plasma with  $r < r_0$  connected to  $\mathbf{B}$  field lines within the sheared layer will be carried along at the same  $\Omega_R$ , but is R-T stable.

The dynamics of the  $n = 2$  instability is of particular concern for MTF because  $\alpha$  increases significantly during wall compression by a cylindrical liner. To see this,  $\Omega_R$  goes as  $r_s^{-2}$  from angular momentum conservation. Meanwhile,  $x_s \equiv r_s/r_c$  is

conserved during wall compression, where  $r_c$  is the liner inner radius (Tuszewski[8], p. 2058). Given this, plasma  $\beta$  is conserved (Tuszewski, Eq. 10). Given *this* and flux conservation,  $\Omega_{Di}$  goes as  $T_i$ , (Shimamura and Nogi[9], Eq. 7 with  $\Omega^* = -\Omega_{Di}$ ). The FRC's characteristic volume  $V = \pi r_s^2 l_s$ , meanwhile, goes as  $r_s^N$ , where  $l_s$  is the separatrix length, and  $N$  is the dimensionality of compression. Assuming adiabatic compression,  $T_i V^{5/3-1} = \text{const}$ . Therefore,  $\Omega_{Di} r_s^{2N/3} = \text{const}$ , and  $\Omega_{Di}$  goes as  $r_s^{-2N/3}$ .  $\alpha$ , then, goes as  $r_s^{-2}/r_s^{-2N/3} = r_s^{-2(1-N/3)}$ .  $N = 12/5$  for wall compression (Tuszewski, Table V), so  $\alpha$  goes as  $r_s^{-2/5}$  or, equivalently,  $r_c^{-2/5}$ . The (target) factor of 10 radial compression, then, increases  $\alpha$  by a factor of  $10^{2/5} \approx 2.5$ .

The general model used to study the development of the FRC's sheared flow layer is more fully developed in a recent publication[10]. We include a brief summary of its relevant results to make this presentation more self-contained. The model is planar with  $\mathbf{x}$ ,  $\mathbf{y}$ , and  $\mathbf{z}$  directions corresponding to  $-\mathbf{r}$ ,  $\boldsymbol{\theta}$ , and  $\mathbf{z}$  of the FRC's cylindrical coordinates, respectively. The reference frame is rotating, with centripetal acceleration providing "gravity"  $g$ . This simplification is employed due to the lack of availability of a cylindrical calculation- that takes into account a magnetically transverse sheared flow layer.

### Rigid rotor case

Before proceeding with the sheared flow model, it is of interest to verify that applying planar theory to the rotational instability of a rigid rotor  $\theta$  pinch and FRC, for which better treatments (as referenced above) *are* available for comparison. To this end, Roberts and Taylor's[11] show that for the (shear free) case where  $\rho_0$  increases with height as  $\exp(\lambda x)$ , R-T modes are stable for magnetically transverse wave numbers  $k$  provided

$$g \leq \nu^2 \lambda k^2 \quad \nu = \frac{k_B T_i}{2ZeB} \quad (2)$$

$\nu$  is the "gyroviscosity" coefficient with  $k_B$ ,  $e$ , and  $B$  being the Boltzmann constant, elementary charge, and magnetic field magnitude, respectively.

To apply this result to a rotating cylindrical plasma column with an axial magnetic field of characteristic magnitude  $B$ , we note that the the ion diamagnetic drift frequency is

$$\Omega_{Di} = -\frac{v_{Di}}{r} \quad \mathbf{v}_{Di} = -\frac{\nabla p_i \times \mathbf{B}}{eZn_i B^2} \quad (3)$$

where  $\mathbf{v}_{Di}$  is diamagnetic drift velocity,  $p_i$  and  $n_i$  are ion pressure and number density, respectively. Using centripetal acceleration for  $g$  at the characteristic radius of the column  $r_0$ , and wrapping the mode “plane” around the circumference, we have, then, the characteristic values,

$$\Omega_{Di} = \frac{2\lambda\nu}{r_0} \quad g = \Omega_R^2 r_0 \quad k = \frac{n}{r_0} \quad \alpha = \frac{\Omega_R}{\Omega_{Di}} \quad (4)$$

From Eq. 2, our stability criterion is, then,

$$\alpha \leq \frac{n}{2\sqrt{\lambda r_0}} \quad (5)$$

For a  $\theta$  pinch, the characteristic density gradient scale length is  $1/\lambda \approx r_0$ , so stability requires  $\alpha \lesssim 1$  for the least stable mode  $n = 2$ . We exclude  $n = 1$  since it results in a bulk lateral acceleration of the plasma column, violating linear momentum conservation, so the model cannot be applied. An FRC’s density peaks near the magnetic axis at  $r = r_0$ , so we take  $1/\lambda \approx (r_s - r_0)$  for this. We have, then, for FRC stability,

$$\alpha \leq \frac{n}{2\sqrt{A}} \quad A = \frac{r_0}{r_s - r_0} \quad (6)$$

$A$  is a measure of the FRC aspect ratio, typically 2 to 3 ( $\alpha \lesssim 0.57\text{--}0.71$ ).

These critical values are close enough to those of the more sophisticated modeling referenced to proceed with a degree of confidence in the semi-quantitative usefulness of a planar model applied to the rotational instability, in addition to providing an alternate explanation or, at least, an addition reason for an FRC’s lower critical  $\alpha$ .

### Sheared flow model

We assume a perfectly conducting isothermal  $z$  invariant plasma with a magnetic field of magnitude  $B$  in the  $\mathbf{z}$  direction, and a uniform gravitational field of magnitude  $g$  in the  $-\mathbf{x}$  direction. For incompressible motion confined to the  $x - y$  plane, the MHD equation of motion supplemented by the isothermal transverse contribution to the FLR stress tensor  $\mathbf{\Pi}$  given by Hazeltine and Meiss[12], Chap.

6, Eq. 123, along with the equations of continuity and state are

$$\begin{aligned}
\rho \partial \mathbf{v} / \partial t + \rho (\mathbf{v} \cdot \nabla) \mathbf{v} &= -\nabla p^* - g \rho \mathbf{x} - \nabla \cdot \mathbf{\Pi} & \partial \rho / \partial t + \nabla \cdot (\rho \mathbf{v}) &= 0 \\
\nabla \cdot \mathbf{v} &= 0 & p^* \equiv k_B T \rho / m_i + B^2 / (2\mu_0) & \nu = k_B T_i / (2ZeB) & T \equiv (T_i + ZT_e) \\
-(\nabla \cdot \mathbf{\Pi}) \cdot \mathbf{x} &= \frac{\partial}{\partial x} \left[ \nu \rho \left( \frac{\partial v_y}{\partial x} + \frac{\partial v_x}{\partial y} \right) \right] - \frac{\partial}{\partial y} \left[ \nu \rho \left( \frac{\partial v_x}{\partial x} - \frac{\partial v_y}{\partial y} \right) \right] \\
-(\nabla \cdot \mathbf{\Pi}) \cdot \mathbf{y} &= -\frac{\partial}{\partial y} \left[ \nu \rho \left( \frac{\partial v_y}{\partial x} + \frac{\partial v_x}{\partial y} \right) \right] - \frac{\partial}{\partial x} \left[ \nu \rho \left( \frac{\partial v_x}{\partial x} - \frac{\partial v_y}{\partial y} \right) \right]
\end{aligned} \tag{7}$$

$\mathbf{v}$ ,  $\rho$ ,  $m_i$ , and  $\mu_0$  are velocity, density, ion mass, and free space permeability, respectively.

The equilibrium states of interest have  $\mathbf{v} = V(x) \mathbf{y}$ ,  $\rho = \rho_0(x)$ ,  $\mathbf{B} = B_0(x) \mathbf{z}$ , and  $\nu = \nu_0(x)$ . For instabilities with short wavelengths relative to the sheared flow layer thickness, consider case I of two semi-infinite regions separated at  $x = 0$  with equilibrium conditions

$$\begin{aligned}
\rho_0 &= \rho_1 & V &= s_1 x & \nu_0 &= \nu_1 & \text{if } x < 0 \\
\rho_0 &= \rho_2 & V &= s_2 x & \nu_0 &= \nu_2 & \text{if } x \geq 0
\end{aligned} \tag{8}$$

where  $\rho_1$ ,  $\rho_2$ ,  $s_1$ ,  $s_2$ ,  $\nu_1$ , and  $\nu_2$  are constants. Assuming shear factors within bounds easily met in fusion research relevant FRC's ( $s \ll 4ZeB / (\beta_i m_i)$ , where  $\beta_i$  is the ion pressure to magnetic pressure ratio), the condition for linear instability of a perturbation with  $\exp(i\omega t + ik y)$  dependence, implying maximum growth rate  $\gamma = \max(-\text{Im} \omega)$ , is

$$\begin{aligned}
J^* > \frac{(1-G^*K^2)^2}{2K} \rightarrow \Gamma = \sqrt{1 - \frac{(1-G^*K^2)^2}{2J^*K}} & J^* \equiv \frac{g^*}{s^{*2}d} & G^* \equiv \frac{\nu^*}{2s^{*2}d^2} & \Gamma \equiv \frac{\gamma}{\sqrt{g^*k}} \\
K \equiv 2kd & \nu^* = \frac{\nu_2 \rho_2 - \nu_1 \rho_1}{\rho_1 + \rho_2} & s^* = \frac{s_2 \rho_2 - s_1 \rho_1}{\rho_1 + \rho_2} & g^* = g \frac{\rho_2 - \rho_1}{\rho_1 + \rho_2}
\end{aligned} \tag{9}$$

Here,  $2d$  is the thickness of the plasma layer intended to be modeled. An R-T relevant configuration is one for which  $\rho_2 > \rho_1$ , implying positive  $J^*$ .  $G^*$  may be of either sign regardless of the relative magnitudes of  $\rho_1$  and  $\rho_2$ . The global stability criterion is

$$J^* \leq \begin{cases} 8\sqrt{-G^*/27} & \text{if } G^* < 0 \\ 0 & \text{if } G^* \geq 0 \end{cases} \tag{10}$$

Note that an R-T relevant configuration is unstable if  $G^* > 0$ , and gyroviscosity suppresses the stabilizing influence of flow shear in the vicinity of  $K = 1/\sqrt{G^*}$ .

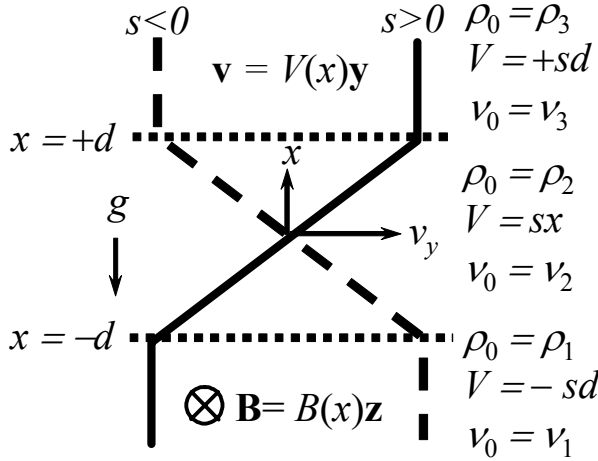


Fig. 1 Geometry and coordinate system assumed for case II - a flow sheared layer separating two unsheared semi-infinite regions. The  $\otimes$  “tail feathers” symbol indicates the magnetic field direction is into the page. The solid/dashed  $V$  vs.  $x$  plot corresponds to a positive/negative shear factor  $s$ , given the coordinate conventions.

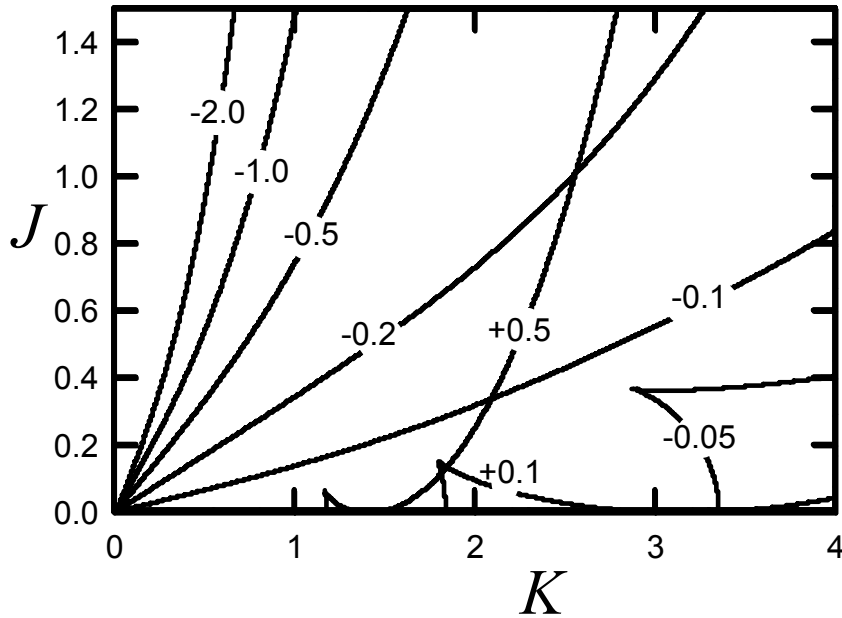


Fig. 2 Stability boundaries for case II with  $\epsilon_1 = \epsilon_3 = 0$  for various values of  $G_2$ , as labeled on the individual plots. The stable region is to the right and below

each contour. Note for  $G_2 > 0$ , the value of  $K$  unstable for all  $J$  is  $K = 1/\sqrt{G_2}$ , the same as with case I with  $G^* = G_2$ .

For case II, we assume three regions of uniform  $\rho_0$  and  $\nu_0$  with equilibrium properties identified by subscripts 1, 2, and 3. We restrict uniform flow shear to the intermediate region of thickness  $2d$ , and drop the “\*” superscripts used to generalize the results. As illustrated in Fig. 1, In equilibrium,

$$\begin{aligned} \rho_0 = \rho_1 & & V = -sd & & \nu_0 = \nu_1 & \text{if} & & x < -d \\ \rho_0 = \rho_2 & & V = sx & & \nu_0 = \nu_2 & \text{if} & & -d < x < +d \\ \rho_0 = \rho_3 & & V = +sd & & \nu_0 = \nu_3 & \text{if} & & x > +d \end{aligned} \quad (11)$$

The linear dispersion relation this time is a quartic  $\omega$  with solutions parameterized by

$$K \equiv 2kd \quad J \equiv \frac{g}{s^2d} \quad G_i \equiv \frac{\nu_i}{2sd^2} \quad \epsilon_i \equiv \frac{\rho_i}{\rho_2} \quad (12)$$

Figure 2 plots the stability boundaries for  $\epsilon_1 = \epsilon_3 = 0$  for a  $G_2$  range relevant to FRC's. This represents a plasma layer accelerated by a  $\mathbf{B}$  field. It is generally found that if the application of case I to either interface of case II results in  $G^* > 0$  with least stable mode  $K = 1/\sqrt{G^*}$ , case II plots are consistent with this result. That is, the finite thickness of the shear layer doesn't change this result, so case I may be used to provide guidance.

### FRC application

We now relate this model to an FRC with an outer layer of plasma with sheared toroidal flow. Taking the exterior pressure scale length in Eq. 3 to be  $(r_s - r_0)$ , we take the characteristic  $\Omega_{Di}$  to be, with the help of Eqs. 7,

$$\Omega_{Di} = \frac{2A\nu}{r_0^2} \quad r_s = r_0 \frac{1+A}{A} \quad (13)$$

where  $A$  is the aspect ratio, as defined in Eqs. 6. Consider now a sheared flow layer that has diffused distance  $2d$  into the FRC. The angular velocity is  $\Omega_R$  at  $r = r_s$ , dropping to zero at  $r = r_s - 2d$ . One shortcoming of applying the planar model to an FRC is that centripetal acceleration depends on  $r$ , while the model assumes  $g$  is constant. With the understanding that we are only seeking rough estimates of global (low  $n$ ) mode behavior, we'll take the characteristic  $g$  to be half its surface value. And, since  $g$  goes as  $\Omega^2$ , we'll take the characteristic angular velocity for the purposes of defining  $\alpha$  to be  $\Omega_R/\sqrt{2}$ ,

$$g = \frac{\Omega_R^2 r_s}{2} \quad \alpha \equiv \frac{\Omega_R}{\sqrt{2}\Omega_{Di}} \quad (14)$$

It should be emphasized that these expressions are only appropriate for low order  $n$  modes which are not localized to either inner or outer boundary. The characteristic  $g$  will be somewhat higher for high order modes localized to the outer surface, and lower for interior modes.

From Fig. 1, the surface velocity is  $2V = -\Omega_R r_s$ , and the layer's shear factor is  $s = V/d$ . So, with the help of Eqs. 13,

$$\Omega_R = -\frac{sA}{A^*(1+A)} \quad A^* = \frac{r_0}{2d} \quad (15)$$

Where  $A^*$  is the aspect ratio of the sheared layer. From Eqs. 13 and Eqs. 14, then,

$$G_2 \equiv \frac{\nu}{2sd^2} = -\frac{A^*}{\sqrt{2}\alpha(1+A)} \quad (16)$$

This provides  $G_2$  for case II, and a way to find  $G^*$  for case I as applied to the *inner* shear layer boundary. Note that for an FRC,  $\Omega_R$  develops with the same sign as  $\Omega_{Di}$ [13] ( $\alpha > 0$ ). Therefore,  $s$  and  $G_2$  here are negative.

From Eqs. 14 and Eqs. 15,

$$J = \frac{g}{s^2d} = \frac{A}{A^*(1+A)} \quad (17)$$

This provides  $J$  for case II. Meanwhile, to relate mode number  $n$  to the model, we use  $k = n/r_0$ . From Eqs. 15, then,

$$K = 2kd = \frac{n}{A^*} \quad (18)$$

### Thin shear layer

As an application of case I, consider a shear layer represented by region 1 which has diffused a small distance into the FRC ( $A^* \gg A$ ). The FRC interior to this layer is taken to be region 2 with  $s_2 = 0$  and a higher density than region 1 of, say,  $\rho_2 = 2\rho_1$ .  $B$  is fairly uniform in the vicinity of interest, so  $\nu_2 = \nu_1$  is assumed. From Eqs. 9,

$$\nu^* = \frac{\nu_1}{2} \quad s^* = -\frac{s_1}{3} \quad g^* = \frac{g}{3} \quad J^* = 3 \left( \frac{g}{s_1^2 d} \right) \quad G^* \equiv -\frac{3}{2} \left( \frac{\nu_1}{2s_1 d^2} \right) \quad (19)$$

$s_1$  equals case II's  $s$ , so  $s_1 < 0$  and, therefore,  $G^* > 0$ . From Eq. 10, then, the configuration is unstable with fully destabilized mode  $K = 1/\sqrt{G^*}$ . From Eqs. 19, Eq. 16, and Eq. 18, this corresponds to

$$n = \sqrt{\frac{2\sqrt{2}}{3}} \sqrt{\alpha A^* (1 + A)} \approx \sqrt{\alpha A^* (1 + A)} \quad (20)$$

For example, if  $A = 2$ ,  $A^* = 10$ , and  $\alpha = 1$ , the least stable mode is  $n = 5$ .

The FRC must survive this turbulent period where unstable modes become of increasingly lower order as the FRC settles down and  $A^*$  decreases. Experimental conditions for this to occur successfully are determined empirically. Framing camera images in visible light during the early  $\theta$  pinch phase of FRC formation[14], and in VUV during early reversal[15] often show high order mode activity, for which the above model may provide a qualitative description. Convective transport of angular momentum toward the interior can be expected on an MHD time scale until the shear layer reaches  $r = r_0$  ( $A^* = A$ ), where  $\mathbf{B}$  reverses and  $G^* > 0$ , therefore, is no longer the case. We treat this phase below.

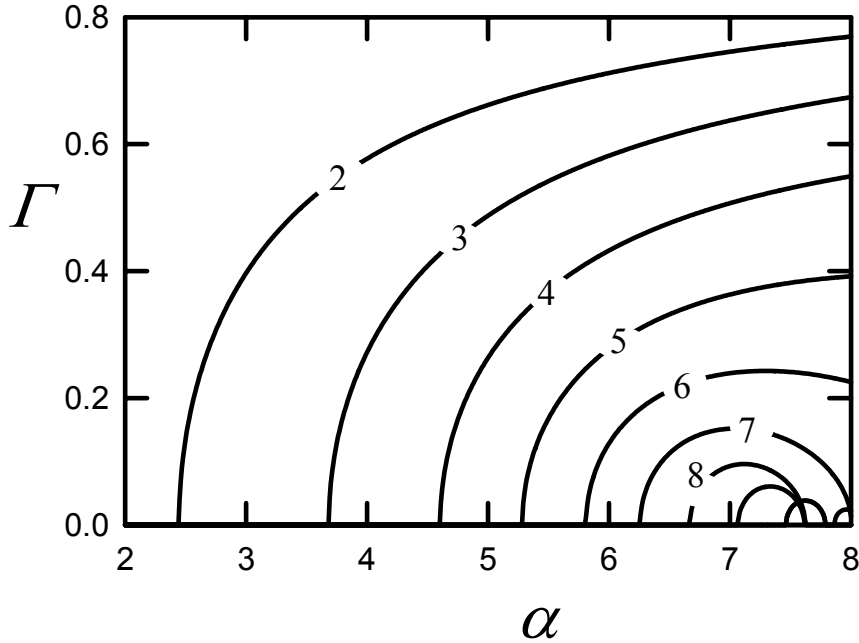


Fig. 3 Normalized growth rate  $\Gamma$  vs  $\alpha$  for various modes  $n$  (labeled) for  $A = 2$ .

### Thick shear layer

Assuming the sheared layer diffuses to  $r_0$  ( $A^* = A$ ), case II parameters are, from Eq. 16, Eq. 17, and Eq. 18,

$$G_2 = -\frac{A}{\sqrt{2}\alpha(1+A)} \quad J = \frac{1}{(1+A)} \quad K = \frac{n}{A} \quad (21)$$

Figure 3 illustrates the normalized growth rate vs.  $\alpha$  for the first several modes with  $A = 2$ . These curves have a very weak dependence on  $A$ , though, for low  $n$ . The stability threshold for  $n = 2$  in the range  $1 \leq A \leq 4$  is  $\alpha = 2.5 \pm 0.1$ .

### Conclusions

A plausible mechanism is presented to explain why the critical  $\alpha$  for stability  $\alpha_{\text{crit}}$  observed for FRC's is significantly higher than that predicted by rigid rotor hybrid simulations of an elongated FRC. In so doing, an alternate or additional reason (density profile differences) is presented for the lower  $\alpha_{\text{crit}}$  found in rigid rotor simulations of an FRC vs. a  $\theta$  pinch. While a rigidly rotating FRC can be expected to have  $\alpha_{\text{crit}} \approx 0.5$ , one that develops a sheared toroidal flow distributed between the separatrix and magnetic axis can theoretically achieve  $\alpha_{\text{crit}} \approx 2.5$ , based on the simplified planar model presented. Furthermore, such a layer should spontaneously develop due to the convection of angular momentum from an initially unstable thin sheared layer set up by kinematic viscosity in concert with angular momentum transport mechanisms theorized to occur outside the separatrix.

### References

- [1] J. P. Freidberg and L. D. Pearlstein, *Phys. Fluids* **21**, 1207 (1978).
- [2] C. E. Selyer, *Phys. Fluids* **22**, 2324 (1978).
- [3] D. S. Harned, *Phys. Fluids* **26**, 1320 (1981).
- [4] Y. Ito, M. Tanjyo, S. Ohi, G. S., and T. Ishimura, *Phys. Fluids* **30**, 168 (1987).
- [5] L. Spitzer Jr., *Physics of Fully Ionized Gases* (John Wiley & Sons, New York, NY, 1967).

- [6] T. Intrator, S. Y. Zhang, J. H. Degnan, I. Furno, C. Grabowski, S. C. Hsu, E. L. Ruden, P. G. Sanchez, J. M. Taccetti, M. Tuszewski, W. J. Waganaar, and G. A. Wurden, *Phys. Plasmas* **11**, 2580 (2004).
- [7] L. C. Steinhauer, *Phys. Fluids* **24**, 328 (1981).
- [8] M. Tuszewski, *Nuclear Fusion* **28**, 2033 (1988).
- [9] S. Shimamura and Y. Nogi, *Fusion Tech.* **9**, 69 (1978).
- [10] E. L. Ruden, *Phys. Plasmas* **11**, 713 (2004).
- [11] K. V. Roberts and J. B. Taylor, *Phys. Rev. Lett.* **8**, 197 (1962).
- [12] R. D. Hazeltine and J. D. Meiss, *Plasma Confinement* (Addison-Wesley, Redwood, CA, 1992).
- [13] M. Tuszewski, *Phys. Fluids B* **2**, 2541 (1990).
- [14] T. P. Intrator, J. Y. Park, J. H. Degnan, I. Furno, C. Grabowski, S. C. Hsu, E. L. Ruden, P. G. Sanchez, J. M. Taccetti, M. Tuszewski, W. J. Waganaar, G. A. Wurden, S. Y. Zhang, and Z. Wang, *IEEE Trans. on Plasma Sci.* **32**, 152 (2004).
- [15] D. P. Taggart, R. J. Gribble, A. D. Bailey III, and S. Sugimoto, in *US-Japan Workshop on Field-Reversed Configurations with Steady-State High-Temperature Fusion Plasmas and the 11'th US-Japan Workshop on Compact Toroids*, edited by D. C. Barnes, J. C. Fernández, and D. J. Rej (LANL, LA-11808-C, Los Alamos, NM, 1994), pp. 87–92.